Isoform-Selective Disruption of AKAP-Localized PKA Using Hydrocarbon Stapled Peptides

Yuxiao Wang,[†] Tienhuei G. Ho,[†] Daniela Bertinetti,[‡] Matthias Neddermann,[‡] Eugen Franz,[‡] Gary C. H. Mo,[§] Lewis P. Schendowich,[†] Avinash Sukhu,[†] Raybun C. Spelts,[†] Jin Zhang,[§] Friedrich W. Herberg,[‡] and Eileen J. Kennedy*[,†]

[†]Department of Pharmaceutical and Biomedical Sciences, College of Pharmacy, University of Georgia, Athens, Georgia 30602, United States

[‡]Department of Biochemistry, University of Kassel, 34132 Kassel, Germany

[§]Department of Pharmacology and Molecular Sciences, The Johns Hopkins University School of Medicine, Baltimore, Maryland 21205, United States

S *Supporting Information*

ABSTRACT: A-kinase anchoring proteins (AKAPs) play an important role in the spatial and temporal regulation of protein kinase A (PKA) by scaffolding critical intracellular signaling complexes. Here we report the design of conformationally constrained peptides that disrupt interactions between PKA and AKAPs in an isoform-selective manner. Peptides derived from the A Kinase Binding (AKB) domain of several AKAPs were chemically modified to contain an all-hydrocarbon staple and target the docking/dimerization domain of PKA-R, thereby occluding AKAP interactions. The peptides are cell-permeable against diverse human cell lines, are highly isoform-selective for PKA-RII, and can effectively inhibit interactions between AKAPs and PKA-RII in intact cells. These peptides can be applied as useful reagents in cell-based studies to selectively disrupt AKAP-localized PKA-RII activity and block AKAP signaling complexes. In summary, the novel hydrocarbon-stapled peptides developed in this study represent a new class of AKAP disruptors to study compartmentalized RII-regulated PKA signaling in cells.
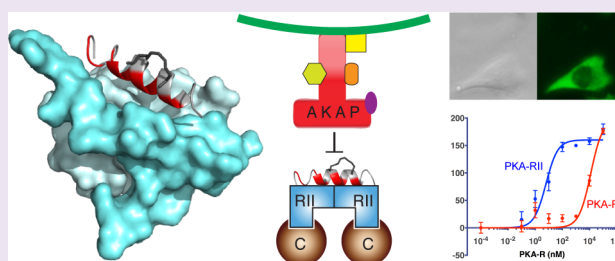
Protein kinase A (PKA), or cAMP-dependent protein kinase, has broad substrate specificity and regulates a myriad of highly diverse cellular processes. Multiple mechanisms exist to fine-tune the spatial and temporal regulation of PKA on subcellular signaling.[1−3] The PKA holoenzyme complex is a tetramer composed of two catalytic subunits (PKA-C) and a regulatory subunit dimer (PKA-R). When intracellular cAMP levels increase, the PKA-R subunits bind cAMP and undergo a conformational change to release the catalytic subunits, which then perform substrate phosphorylation.[4,5] Regulation of PKA activity is partly controlled through the utilization of four distinct PKA-R subunit isoforms: PKA-RI (RIα and RIβ) and PKA-RII (RIIα and RIIβ). The PKA-R isoforms differ in many aspects including tissue expression, cAMP sensitivity, and intracellular localization.[1]

PKA activity is further regulated by a class of proteins called A kinase-anchoring proteins (AKAPs).[3,6] The AKAP family is structurally diverse but shares the commonality of binding to PKA-R and compartmentalizing the PKA holoenzyme to multiple subcellular locations including the plasma membrane, endoplasmic reticulum, and mitochondria.[3] AKAPs act as scaffolding proteins that tether PKA along with other proteins so as to integrate PKA activity into distinct multivalent signaling complexes. Other proteins tethered to these subcellular complexes include kinases, phosphatases, adenylyl cyclases, phosphodiesterases, and various substrates.[7−9] By confining PKA to subsets of cellular substrates within a local cAMP environment, AKAPs provide intrinsic specificity to cAMP-PKA signaling pathways and therefore act as key regulators for various cellular processes (Figure 1a).[3,6] While most AKAPs preferentially bind to PKA-RII, several AKAPs have been identified that have PKA-RI specificity or can bind both PKA-RI and PKA-RII (dual specific).[10,11] Isoform-selective interactions appear to be critical for AKAP-mediated signaling since altered interactions between AKAPs and the PKA-R isoforms correlate with misregulated PKA activity and various disease states.[12]

The significance of AKAP regulation on PKA activity is further underscored by its correlation with various disease phenotypes. Altered AKAP activity is implicated in many pathological processes including cardiovascular disorders, immune diseases, and multiple cancer phenotypes.[13−15] While AKAPs are clearly important regulators of PKA, their full biological roles are largely elusive due to the complex nature of
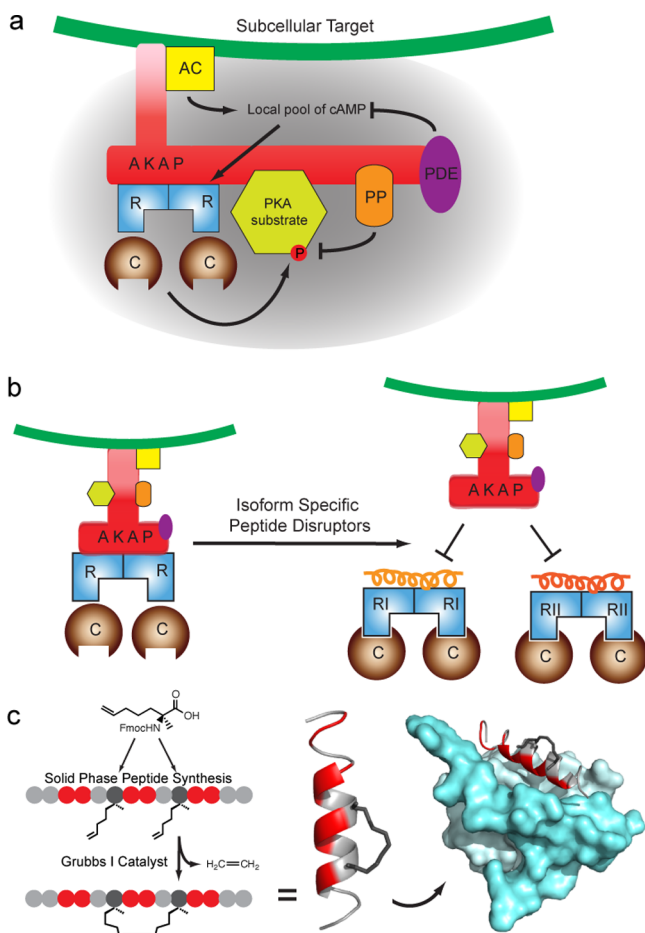
Figure 1. RII-selective disruption of AKAP-mediated PKA anchoring using hydrocarbon-stapled peptides. (a) AKAPs regulate the phosphorylation of PKA substrates in a spatiotemporal manner by recruiting related machinery to subcellular locations for compartmentalized signaling. (b) Isoform-selective peptides were designed to mimic the AKB helix from AKAP that binds PKA-R. Peptides can be engineered to have specificity toward either isoform of PKA-R, thereby blocking downstream signaling through displacement of PKA-R from the AKAP signaling complex. (c) Pairs of the non-natural amino acid S$_5$ (shown in dark gray) are introduced into AKB or AKB-like sequences at i and $i + 4$ positions. A hydrocarbon staple is formed by ring-closing olefin metathesis to form the conformationally constrained product. The hydrophobic residues that are essential for PKA-AKAP interactions (shown in red) were left unchanged. The engineered stapled peptide will target the AKB-binding site on the surface of the docking/dimerization (D/D) domain of PKA-RII (shown in blue). Structure rendered in PyMol using PDB ID 2HWN.[24]

spatial and temporal regulation. In order to elucidate the role of AKAPs on localized PKA signaling, significant efforts have been put forth to block interactions between PKA and AKAP in a highly isoform-selective manner (Figure 1b). One of the first peptide disruptors, Ht31, was derived from AKAP-Lbc and was subsequently modified to contain a stearated moiety to allow for cell permeability.[16] Other peptides were also developed with improved properties including greater isoform specificity or higher binding affinities such as RIAD (RI-anchoring disruptor)[17] and SuperAKAP-IS.[10] Collectively, these peptides have become valuable tools to block PKA signaling mediated by either PKA-RI or PKA-RII PKA. However, there are still limitations with the physical properties of these compounds

including poor cellular uptake by intact cells, loss of the secondary structural fold in solution, and susceptibility to proteolytic degradation that is intrinsic to nonmodified peptidyl bonds. Various modifications including addition of stearic acid[18] and additions of either a poly arginine tag or HIV-1 TAT sequences[19,20] have been utilized to improve cellular permeability. Nevertheless, many limitations still exist using these synthetic strategies including lack of reinforced secondary structure in solution, relatively short half-life values, and potential mislocalization caused by the addition of conjugated sequences or moieties.

As an alternative strategy for the development of isoform-selective AKAP disruptors, we applied hydrocarbon peptide stapling. This chemical modification constrains the secondary structure of α-helices through α-methylation and macrocyclic ring formation (Figure 1c).[21] Further, this modification was found to increase the proteolytic stability of the peptide while also making it more entropically favorable for binding by locking it in a prebinding state.[22] As a strategy to disrupt AKAP interactions, we focused on the conserved AKB helix that is shared among AKAPs. The AKB binds to the docking/dimerization (D/D) domain of PKA-R that is formed at the PKA-R dimer interface.[23] Crystallographic studies show that interactions between the amphipathic AKB peptides and the D/D domain of either PKA-RI or PKA-RII are predominantly driven by hydrophobic interactions.[24,25] Many AKB or AKB-like sequences have been previously identified; however, the majority of these sequences are highly hydrophobic and therefore are limited in their potential as biochemical tools. We chose three intrinsically more hydrophilic sequences that target the AKB binding and used these as templates for generating hydrocarbon stapled peptide inhibitors: RIAD, AKAP220, and small membrane AKAP (smAKAP). In addition, the nonmodified AKB sequences inherently have specificity for either PKA-RI or PKA-RII, thereby providing a basis for PKA-R isoform selectivity (Figure 1b). Non-natural olefinic amino acids ((S)-2-(4′-pentenyl)alanine), abbreviated as S$_5$, were introduced into the peptide sequences in the i, $i + 4$ positions (Figure 1c). The olefinic amino acids were covalently cross-linked using ring-closing metathesis chemistry.[26,27] Libraries were generated where N- and C-terminal truncations were made to shorten the AKB sequence while preserving the hydrophobic residues of the binding interface (Figure 2, parent sequences). The hydrocarbon staples were introduced into various positions of the sequence by introducing the non-natural amino acids into positions on the solvent-exposed face of the helix (black residues). However, after introduction of the hydrocarbon staple into the parent sequences, these peptides had poor water solubility and therefore demonstrated minimal cell permeability (Supplementary Figure 1). To remedy the limited cell permeability and solubility of these peptides, the AKB peptide mimics were optimized to increase their amphipathic properties through the addition of hydrophilic Lys residues on the solvent-exposed face of the helix (Figure 2, Lys-modified sequences). In addition, a short (PEG)$_3$ group was added to the N-terminus of the Lys-modified sequences to further improve water solubility.

Next, the binding affinities of the Lys-modified stapled peptides were measured using fluorescence polarization (FP) assays. Peptides were screened against the D/D domains of either RIα or RIIα (Figure 3a and Supplementary Figures 2–4). The Lys-modified sequence lacking the addition of a hydrocarbon staple for each sequence was used as a control. Of
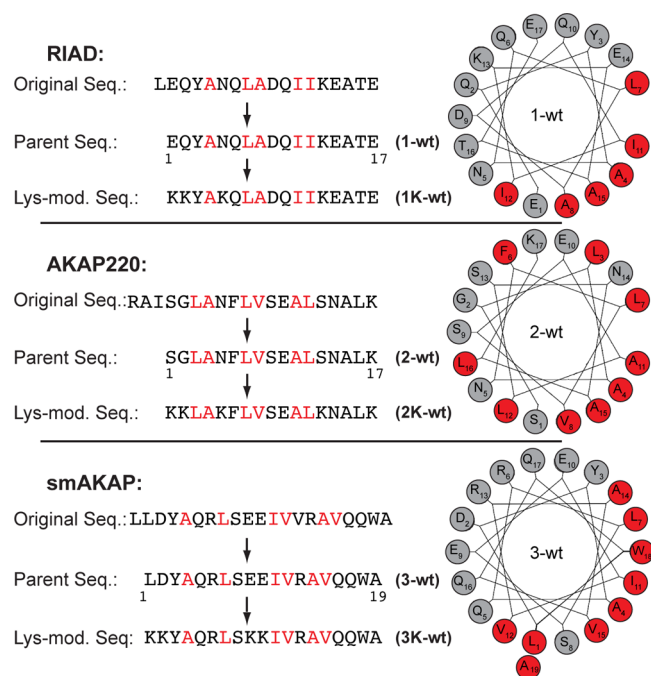
Figure 2. Sequences for design of stapled peptides. Original AKB or AKB-like sequences were slightly shortened to yield the parent sequences for the compound library. Optimization of the sequence was performed to increase the amphipathic properties and water solubility of the sequences, rendering the Lys-modified sequence libraries. Helical wheels of the parent sequences demonstrate the hydrophobic nature of the binding surface. The hydrophobic residues are shown in red and were left unchanged. Non-natural amino acids and Lys residues were introduced on the solvent-exposed hydrophilic surface.

the stapled peptides tested, none had an appreciable binding affinity for the PKA-RI subunit. Although the unmodified, original sequence of RIAD and smAKAP both demonstrate preferential binding to PKA-RI,[12,17] the chemically modified peptides are not as inherently flexible and therefore may have altered binding properties including their entropic and enthalpic properties. Nevertheless, multiple candidates were found that were highly selective for PKA-RII binding. Indeed, almost all of the peptides bearing a hydrocarbon staple at various positions were found to increase the binding affinity for PKA-RIIα. Among all of the Lys-modified peptides tested, three were found that demonstrated K_D values in the low nM range: 1K-3 (2 nM), 2K-3 (6.2 nM), and 3K-5 (2.1 nM). Further, 1K-3 showed weak binding of PKA-RIα in the submicromolar range, while 2K-3 and 3K-5 showed no appreciable binding affinities to PKA-RIα. These three promising candidates for highly selective disruption of PKA-RII were subsequently renamed Stapled Anchoring Disruptors (STADs; 1K-3 is STAD-1, 2K-3 is STAD-2, and 3K-5 is STAD-3). Stapled scrambled controls were also examined for each STAD peptide.

Next, the K_D values were measured for the three STAD peptides using full-length constructs human PKA-R (RIα, RIβ, RIIα, and RIIβ) since this would provide a more relevant portrayal of binding affinities and selectivity in the context of human cells (Figure 3b and c). Each of the isoforms was purified as previously described[28] and tested over a concentration range from 0.1 nM to 15 μM. While all three peptides were found to have K_D values of 50 nM or less for PKA- RIIα, STAD-1 also had a comparable affinity for PKA-RIα (93 nM). However, STAD-2 and STAD-3 interacted more

weakly with PKA-RIα with STAD-2 having a K_D value of greater than 1 μM and STAD-3 having a value of 144 nM. STAD-3 had the lowest K_D values for PKA-RII (8 nM for RIIα and 16 nM for RIIβ). However, STAD-2 has a slightly reduced affinity compared to STAD-3 for PKA-RII (31 nm for RIIα versus 64 nM for RIIβ) but has higher PKA-RII selectivity since STAD-2 binding to PKA-RIIα is approximately 40 times more favorable than for PKA-RIα. Thus, it appears that STAD-2 and STAD-3 have the most pronounced isoform selectivity against full-length human constructs of PKA-RII by approximately 1−2 orders of magnitude as compared to PKA-RI.

With isoform selectivity and low K_D values confirmed, we next wanted to test the cellular uptake of these compounds. Three highly diverse human cell lines (HeLa, MDA-MB-231, and PC-3 cells) were treated with 5 μM 5(6)-carboxyfluorescein-labeled peptides for 6 h before washing and fixation (Figure 4a and Supplementary Figures 5−7). While the nonstapled wild type control peptides for each peptide class were virtually impermeable to each of the cell types, STAD-1, STAD-2, and STAD-3 showed considerable intracellular access in all three cell lines. Further, although some punctate staining is evident, likely indicating intracellular localization in vesicles, particularly for STAD-3, there is a considerable amount of peptide localized in the cytoplasm that would therefore be accessible to AKAP-PKA complexes. Of note, the original and stapled parent sequences were not cell-permeable even after addition of a hydrocarbon staple (Supplementary Figure 1); however, the stapled STADs and their scramble control peptides were all cell-permeable (Figure 4a and Supplementary Figure 8). These observations indicate that addition of Lys residues on the hydrophilic face of the peptide was needed to promote cellular uptake of the peptide sequences.

Since the peptides appeared to have appreciable cytoplasmic localization, we wanted to determine whether they were physically interacting with PKA-R within the intracellular environment. In order to test this, we performed immunoprecipitation assays using MDA-MB-231 cells (Figure 4b). Biotinylated STAD peptides (1 μM) were added to the cell media 1 h before lysis. Cells that were not peptide-treated were used as a control. Pull-downs were performed, followed by immunoblotting for either PKA-RI or PKA-RII. It is clear that both STAD-2 and STAD-3 interact with PKA-RII, while STAD-1 was found to weakly associate with PKA-RII in cells. None of the peptides appear to have any affinity for PKA-RI within cells. This experiment confirms that the STAD peptides are highly RII-selective even within the context of a cellular environment.

To determine whether the STAD peptides can effectively block PKA signaling in cells, we monitored PKA substrate phosphorylation in cells. MDA-MB-231 cells were serum-starved overnight, followed by pretreatment with different concentrations of STAD peptides for 1 h prior to stimulation with 50 μM forskolin (Fsk) to increase cAMP levels. Serum-starvation was performed to downregulate PKA activity so that a robust activation of PKA could be detected upon stimulation of intracellular cAMP levels in the presence or absence of the STAD peptides. PKA activity was measured as a function of substrate phosphorylation using the antiphospho-(Ser/Thr) PKA substrate antibody to detect phosphorylated PKA substrates in MDA-231 cells (Figure 4c). As a control, the small molecule inhibitor H89 (50 μM) was used to inhibit PKA-C activity. Phosphorylation of CREB was also independently monitored since this is a known AKAP-mediated

637

dx.doi.org/10.1021/cb400900r | *ACS Chem. Biol.* 2014, 9, 635−642

a

Peptide	Sequence	RIα(nM)	RIIα(nM)	
1K-wt	KKYAKQLADQIIKEATE	> 1000	605 ± 190	STAD-1 wt
1K-1	K*YAK*LADQIIKEATE	791 ± 237	105 ± 34	
1K-2	KKYAK*LAD*IIKEATE	353 ± 193	123 ± 62	
1K-3	KKYAKQLAD*IIK*ATE	240 ± 56	2.0 ± 0.8	STAD-1
1K-4	KKYAKQLADQII*EAT*	> 1000	232 ± 53	
1K-3-scr	AAEDYKIKI*LKT*QAK	> 1000	> 1000	
2K-wt	KKLAKFLVSEALKNALK	> 1000	22.4 ± 6.1	STAD-2 wt
2K-1	K*LAK*LVSEALKNALK	> 1000	17.6 ± 7.0	
2K-2	KKLAK*LVS*ALKNALK	> 1000	28.7 ± 9.8	
2K-3	KKLAKFLVS*ALS*ALK	> 1000	6.2 ± 2.0	STAD-2
2K-3-scr	KALVKLAAL*KFK*LKS	> 1000	> 1000	
3K-wt	KKYAQRLSKKIVRAVQQWA	> 1000	> 1000	STAD-3 wt
3K-1	K*YAQ*LSKKIVRAVQQWA	> 1000	197 ± 110	
3K-2	KKYAQ*LSK*IVRAVQQWA	> 1000	> 1000	
3K-3	KKYAQRLS*KIV*AVQQWA	> 1000	356 ± 189	
3K-4	KKYAQRLSKKIV*AVQ*WA	> 1000	819 ± 383	
3K-5	KKYAQRLSKKIVRAV*QWA*	> 1000	2.1 ± 0.6	STAD-3
3K-5-scr	RVQKIVLRWKYAASQ*KAK*	> 1000	> 1000	

b

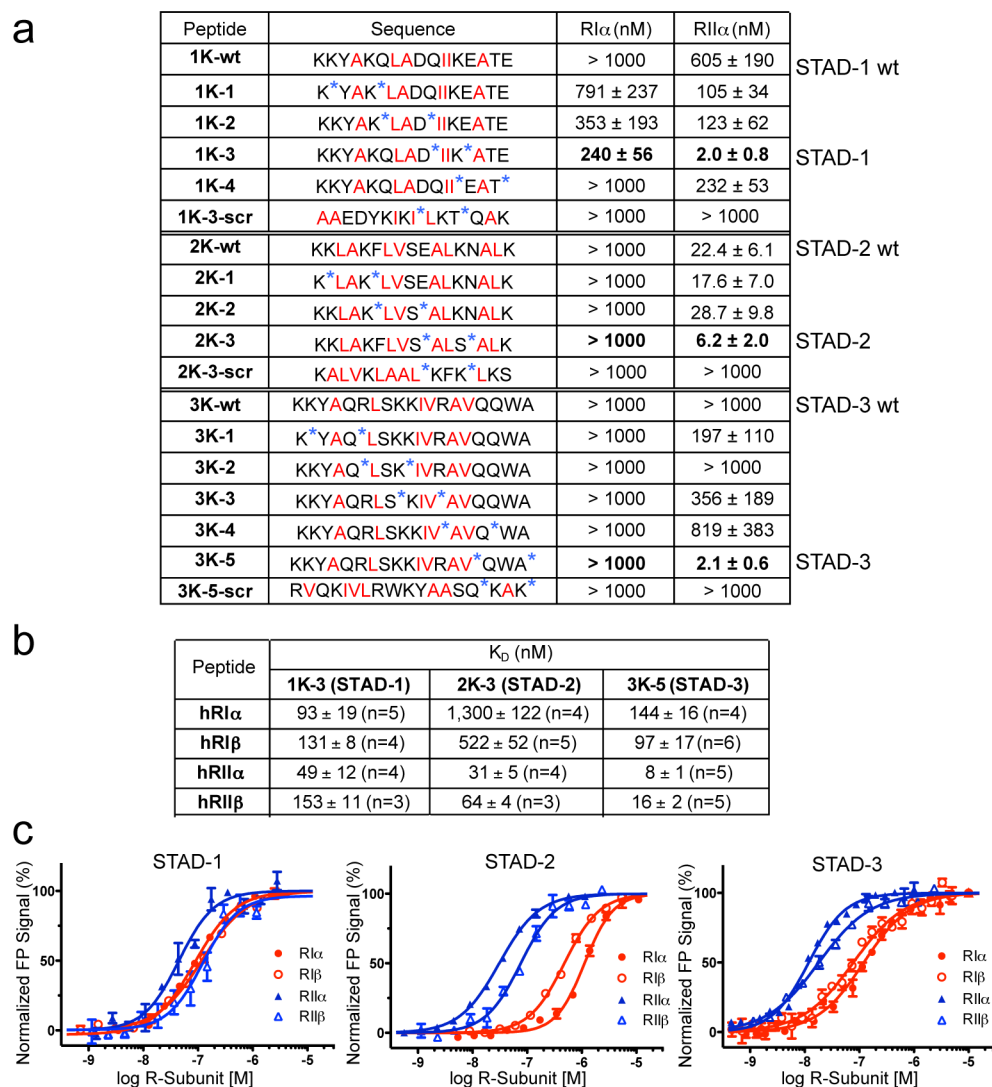| Peptide	K_D (nM)		
	1K-3 (STAD-1)	2K-3 (STAD-2)	3K-5 (STAD-3)
hRIα	93 ± 19 (n=5)	1,300 ± 122 (n=4)	144 ± 16 (n=4)
hRIβ	131 ± 8 (n=4)	522 ± 52 (n=5)	97 ± 17 (n=6)
hRIIα	49 ± 12 (n=4)	31 ± 5 (n=4)	8 ± 1 (n=5)
hRIIβ	153 ± 11 (n=3)	64 ± 4 (n=3)	16 ± 2 (n=5)

c

Figure 3. Stapled peptides are highly selective for the PKA-RII isoform. (a) Fluorescence polarization assays of the Lys-modified peptide libraries were determined using purified protein constructs of the D/D domains from either PKA-RI or PKA-RII. S_5 is represented using blue asterisk symbols. Peptides were plated at a final concentration of 10 nM, and the D/D dimerization domains were tested over a concentration range of 0.1 nM to 100 μM. Dissociation constants were calculated using nonlinear regression and are presented as mean ± standard error of triplicates. 1K-3 (STAD-1), 2K-3 (STAD-2), and 3K-5 (STAD-3) were identified as peptides with low K_D values for PKA-RII and were highly selective for PKA-RII over PKA-RI. (b) Fluorescence polarization was measured using full-length human proteins for each PKA-R isoform. Each single FP experiment was performed in triplicate. While all three peptides tested bound to PKA-RIIα with a K_D value of 50 nM or less, STAD-2 and STAD-3 appear to have the greatest selectivity for PKA-RII binding over PKA-RI. (c) Normalized FP spectra are shown for each of the full-length PKA R subunit isoforms. PKA-RI is represented in red (closed circles = α, open circles = β), and PKA-RII is shown in blue (closed triangles = α, open triangles = β). STAD-2 and STAD-3 show preference for PKA-RII binding by 1−2 orders of magnitude.

substrate of PKA.[29] All three STAD peptides decreased phosphorylation of various PKA substrates in a dose-dependent manner as compared to the forskolin-stimulated positive control. However, STAD-2 and STAD-3 appear to be more effective at inhibiting substrate phosphorylation as well as reducing phospho-CREB levels in these cell-based assays. Furthermore, the effect on substrate phosphorylation is not universal, but rather some substrates are more impacted than others, most notably under the lower 4 μM treatment conditions. This suggests that phosphorylation of substrates that are regulated by signaling complexes involving AKAPs and PKA-RII are disproportionately reduced. To confirm that the peptide sequences are critical for targeted disruption of AKAP signaling complexes, scrambled versions of each STAD peptide were tested using the same assay. All three scrambled peptides

had no apparent inhibitory effect on PKA signaling as measured by PKA substrate phosphorylation as well as phospho-CREB levels (Figure 4d). Taken together, these results suggest that STAD-2 and STAD-3 can be effectively localized within cells and can selectively disrupt AKAP-regulated signaling involving PKA-RII.

As a means of measuring the effects of the STAD peptides on AKAP-anchored versus non-anchored PKA activity, cytosolic PKA activity was probed using the diffusible biosensor AKAR4 in HeLa cells[30] (Figure 4e and f). Cells treated with STAD-2 responded to Fsk (50 μM)/IBMX (100 μM) stimulation with a 15 ± 6% (n = 3) increase in yellow to cyan emission ratio, compared to a 39 ± 3% (n = 9) response from cells treated with the scramble control peptide. Using biosensor pmAKAR4 (targeted by a CAAX sequence), however, we found that
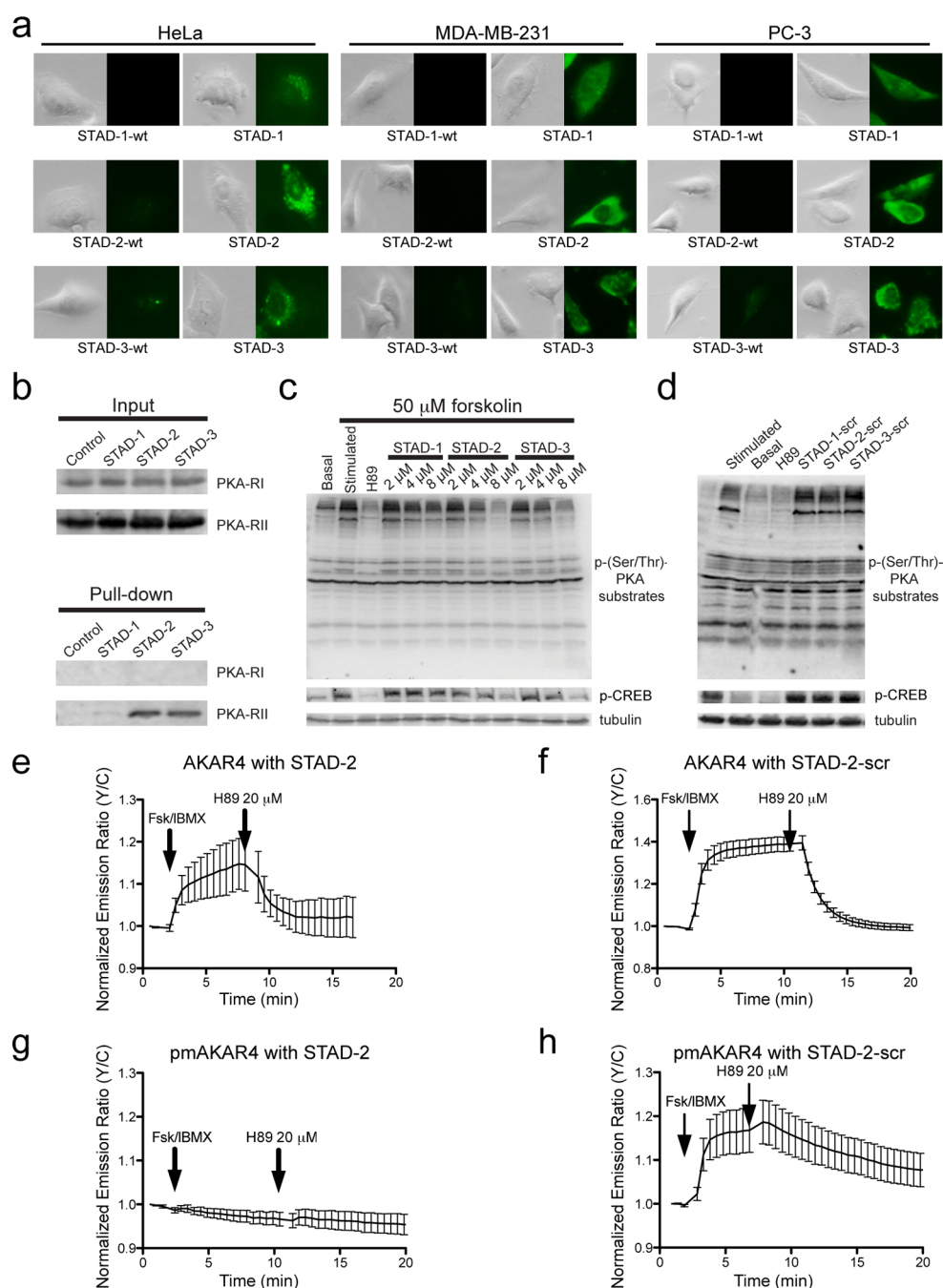
Figure 4. Hydrocarbon stapled peptides selectively bind PKA-RII and disrupt AKAP-mediated PKA signaling in cells. (a) Fluorescent images of diverse cell lines (HeLa, MDA-MB-231, PC-3) after treatment with FITC-labeled peptides (5 μM) for 8 h demonstrates that STAD-1, -2, and -3 are cell-permeable and have at least partial cytosolic localization. Each image is representative of three replicates. (b) Immunoprecipitation experiments were performed in MDA-MB-231 cells. Cells were incubated with N-terminal biotin-labeled peptides (5 μM) and pulled down by avidin-coated resin, and PKA-RI and PKA-RII were detected by immunoblotting. All three peptides demonstrated interactions with PKA-RII to varying degree, while none showed any appreciable affinity for PKA-RI in cells. c) The STAD peptides were found to cause dose-dependent disruption of PKA substrate phosphorylation. Cells were serum-starved, followed by stimulation with 50 μM forskolin (except the basal lane). The PKA inhibitor H89 was used as a control (50 μM). Phosphorylation of CREB was independently monitored to demonstrate that the peptides inhibit a known PKA substrate that is partly regulated by AKAP activity. The image is representative of three independent experiments. (d) STAD scramble peptides (8 μM) were also monitored for their effects on PKA substrate phosphorylation. The scramble control peptides had no effect on PKA substrate phosphorylation or on CREB phosphorylation after forskolin stimulation. (e, f) Cytosolic PKA activity was monitored using the AKAR4 reporter. When treated with either STAD-2 or the STAD-2 scramble control, PKA activity was still stimulated by Fsk (50 μM) and IBMX (100 μM) and inhibited by H89 (20 μM), indicating that STAD-2 does not affect nonlocalized PKA activity. (g, h) PKA activity localized near the plasma membrane was monitored using the pmAKAR4 reporter. In this instance, PKA activity was not stimulated by Fsk/IBMX or inhibited by H89 in the presence of STAD-2, indicating that STAD-2 selectively inhibits localized PKA activity. This effect was not evident when the pmAKAR4 reporter was tested with the STAD-2 scramble control.

STAD-2 could completely inhibit the subpool of PKA located at plasma membrane as compared to a non-peptide-treated control (Figure 4g and Supplementary Figure 9b). The scramble STAD-2 control peptide did not alter the plasma membrane (Figure 4h) PKA responses in HeLa cells.

In summary, we developed conformationally constrained, cell-permeable peptides that are highly selective for disruption of the interactions between AKAPs and PKA-RII. By conformationally constraining these AKAP inhibitor peptides, the binding interface is spatially poised to interact with the D/D of PKA-RII while also decreasing susceptibility to proteolytic degradation.[21] While AKAPs are important regulators of cAMP-mediated signaling in cells, there are still many unknowns regarding their roles in normal and disease-state signaling. This novel class of isoform-selective peptides targeting the AKAP binding site on PKA-R can be utilized as effective tools to selectively disrupt localized signaling complexes mediated by interactions between AKAPs and PKA-RII and block downstream signaling in normal and disease-state cells.

■ METHODS

Materials. The N-α-Fmoc protected amino acids and Rink Amide MBHA Resin were purchased from Novabiochem. (S)-N-Fmoc-2-(4′-pentenyl)alanine was purchased from Okeanos Tech. All other reagents and organic solvents used in this study were purchased from Fisher Scientific except where noted. HPLC grade methanol, acetonitrile, and trifluoroacetic acid were used for all solutions involving preparation or analysis of samples.

Cell Culture. MDA-MB-231 and PC-3 cells were cultured in Roswell Park Memorial Institute-1640 (RPMI) Medium with L-glutamine (Lonza), 10% fetal bovine serum (Thermo Scientific), and penicillin/streptomycin (Amresco). HeLa cells were cultured in Dulbecco's Modified Eagle Medium (DMEM) with glucose and L-glutamine (Lonza), 10% fetal bovine serum (Thermo Scientific), and penicillin/streptomycin (Amresco).

Peptide Synthesis. Peptides were synthesized on Rink Amide MBHA resin using standard 9-fluorenylmethoxycarbonyl (Fmoc) solid phase synthesis. Deprotection steps were performed using a 25% (v/v) solution of piperidine in 1-methyl-2-pyrrolidinone (NMP) for 30 min. For each coupling step, 10 equiv of N-α-Fmoc-protected amino acids (0.25 M final concentration in NMP) were added, followed by addition of 2-(6-chloro-1H-benzotriazole-1-yl)-1,1,3,3-tetramethylaminium hexafluorophosphate (HCTU, 0.23 M final concentration) in NMP and 8% (v/v) N,N-diisopropyl ethylamine (DIEA).

Olefin metathesis was performed using 0.4 equiv bis-(tricyclohexylphosphine) benzylidene ruthenium(IV) dichloride (Grubbs' first generation catalyst, Sigma Aldrich) relative to resin substitution. The reaction was performed in 1,2-dichloroethane at RT for 1 h with agitation. The reaction was repeated once more using the same conditions to ensure complete conversion to the cyclized product. 11-Amino-3,6,9-trioxaundecanoic acid (NH-PEG$_3$-CH$_2$COOH, ChemPep Inc.) was added to the N-terminus of all of the Lys-modified sequences and their scramble controls. The PEG$_3$ group was introduced using standard coupling conditions with 4 equivs before the addition of biotin or 5(6)-carboxyfluorescein. N-Terminal fluorescein labeling was performed using 2 equiv of 5(6)-carboxyfluorescein (Acros Organics) along with 0.046 M HCTU and 2% (v/v) DIEA in N,N-dimethylformamide (DMF) overnight. N-Terminal biotin labeling was performed using 10 equiv of D-biotin (Anaspec), 0.14 M HCTU, and 4% (v/v) DIEA in a 1:1 mixture of DMF and dimethyl sulfoxide (DMSO) overnight. Completed peptides were cleaved from resin using 95% trifluoroacetic acid, 2.5% water, and 2.5% of triisopropylsilane (Sigma Aldrich) for 4−5 h, precipitated in methyl-tert-butyl ether at 4 °C, and lyophilized. All peptides were purified by high-performance liquid chromatography (HPLC) and verified by mass spectrometry (MS). Fluorescein-labeled peptides were

quantified by measuring absorbance of 5(6)-carboxyfluorescein at 495 nm using a Synergy 2 microplate reader (Bio-Tek). Biotin-labeled peptides were quantified by measuring decreased absorbance of the 2-hydroxyazobenzen-4′-carboxylic acid (HABA)-avidin complex (VWR) at 500 nm.

The molecular weights of the purified peptides are as follows: 1K-wt = 2537.4 (expected mass = 2537.8); 1K-1 = 2531.4 (expected mass = 2531.9); 1K-2 = 2531.4 (expected mass = 2531.9); 1K-3 (STAD-1) = 2530.5 (expected mass = 2531.0); 1K-4 = 2530.5 (expected mass = 2530.9); 1K-3-scr (STAD-1 scr) = 2516.1 (expected mass = 2516.9); 2K-wt = 2461.2 (expected mass = 2461.9); 2K-1 = 2436.3 (expected mass = 2436.9); 2K-2 = 2435.1 (expected mass = 2436.0); 2K-3 (STAD-2) = 2454.0 (expected mass = 2455.0); 2K-3-scr (STAD-2 scr) = 2454.0 (expected mass = 2455.0); 3K-wt = 2862.0 (expected mass = 2862.3); 3K-1 = 2827.5 (expected mass = 2828.3); 3K-2 = 2827.5 (expected mass = 2828.3); 3K-3 = 2827.2 (expected mass = 2828.3); 3K-4 = 2828.4 (expected mass = 2828.4); 3K-5 (STAD-3) = 2984.1 (expected mass = 2984.5); and 3K-5-scr (STAD-3 scr) = 2983.4 (expected mass = 2984.5).

Protein Expression and Purification. The RIα docking/dimerization (D/D) domain (residues 1−61) of Bos taurus and the RIIα D/D (1−44) of Rattus norvegicus were expressed as previously described.[24,31] RIα D/D or RIIα D/D cells were suspended and lysed in buffer containing 20 mM Tris (pH 8.0), 100 mM NaCl, and 0.1 mM phenylmethanesulfonylfluoride (PMSF) before purification. The protein constructs were purified using a Talon cobalt-affinity resin (Clontech). Cobalt-purified proteins underwent further purification using a Superdex 75 (10 mm × 300 mm) size exclusion column (AKTA) on an AKTA Purifier UPC 10 (AKTA). Proteins were concentrated using Vivaspin 6 columns with a 3 kDa molecular weight cutoff (GE Healthcare). Proteins were concentrated, and 20% glycerol was added before being snap frozen in liquid nitrogen and stored at −80 °C.

Expression and Purification of Recombinant PKA-R Subunits. Recombinant human PKA regulatory subunits (hRIα, hRIβ, hRIIα, hRIIβ) were expressed and purified as previously described using Sp-8-AEA-cAMPS agarose.[28] SDS-polyacrylamide gel electrophoresis was used to monitor protein expression and purity. Typically, the recombinant proteins were purified to ≥95% homogeneity.

Fluorescence Polarization Using D/D Domain Constructs. Fluorescence polarization (FP) assays were used to measure the binding affinity of designed peptides to the D/D domain of the PKA regulatory subunit isoforms. Each fluorescein-labeled peptide (10 nM) was plated with either RIα D/D or RIIα D/D. The protein constructs were 10-fold serially diluted from 100 μM to 0.1 nM in 10 mM HEPES (pH 7.4), 0.15 M NaCl, 3 mM EDTA, and 0.005% Surfactant P20. The plates were incubated in the dark at RT for 30 min. Fluorescence polarization was measured in triplicate using a Synergy 2 microplate reader (Biotek). Binding curves were generated, and dissociation constants (K_D) were calculated from the nonlinear regression curve using GraphPad Prism.

Fluorescence Polarization Using Full Length PKA-R. To investigate the binding affinity of AKAP peptides to the full-length regulatory subunits of PKA, FP was applied in a direct assay format. Increasing concentrations (from 0.1 nM to 15 μM) of the four different PKA regulatory subunits were mixed with 5−10 nM fluorescently labeled AKAP peptide in 20 mM MOPS pH 7, 150 mM NaCl, 0.005% (v/v) CHAPS. Data were obtained using a FusionTM alpha-FP plate reader at RT and a data acquisition of 2 s at Ex 485 nm/Em 535 nm in a 384 well microtiterplate (Perkin-Elmer Optiplate, black). Data represent the mean ± standard error of the mean of triplicate measurements (n = 3 per data point) for a single experiment. K_D determination was performed as described above.

Cell Permeability Assays. HeLa, MDA-MB-231 or PC-3 cells per well were seeded at 100,000 cells/well on 8-well tissue culture slides (BD Biosciences). Cells were grown overnight in medium with 10% fetal bovine serum. Next, 5 μM 5(6)-carboxyfluorescein-labeled peptides were added and incubated at 37 °C for 6 h before fixation in 2% paraformaldehyde. Slides were imaged using an Olympus X71 fluorescent microscope.

640

dx.doi.org/10.1021/cb400900r | ACS Chem. Biol. 2014, 9, 635−642

Immunoprecipitation Assays. MDA-MB-231 cells were pretreated with 1 μM biotin-labeled peptides before being lysed in NP-40 buffer (20 mM Tris-HCl, pH 8, 137 mM NaCl, 10% glycerol, 1% Nonidet P-40, 2 mM EDTA). Lysates were incubated with 50 μL immobilized avidin resin (G-Biosciences) overnight at 4 °C. The resin was collected by centrifugation at 1000*g for 2 min, washed three times with NP-40 buffer and boiled in Laemmli sample buffer (60 mM Tris-Cl pH 6.8, 2% SDS, 10% glycerol, 5% β-mercaptoethanol, 0.01% bromophenol blue) at 95 °C for 5 min. PKA-RI (1:500, BD Biosciences) and RII (1:1500, Abcam) antibodies were used for Western blot detection. Antirabbit IRDye 800CW (1:25,000) and antimouse IRDye 680LT(1:30,000) secondary antibodies were used (LI-COR Biosciences). Blots were imaged using an Odyssey Fc imaging system (LI-COR Biosciences).

Detection of Phosphorylated PKA Substrates. MDA-MB-231 cells were grown on 12-well culture plate. Cells were serum-starved for 24 h in serum-free RPMI media with glutamine (0.3 g/L). Peptides were added to cell at either 2, 4, or 8 μM concentrations for 1 h, followed by stimulation with 50 μM forskolin for 10 min. As a control, cells were treated with H89 (50 μM) for 30 min prior to forskolin stimulation. Cells were lysed in Laemmli sample buffer and analyzed by Western blotting. Anti-phosphoserine/threonine PKA substrate (1:1000, Cell Signaling Technology) or tubulin (1:2000, DSHB) primary antibodies were used, followed by antirabbit IRDye 800CW (1:25,000) or antimouse IRDye 680LT secondary antibodies (1:30,000) (LI-COR Biosciences). Blots were imaged using an Odyssey Fc imaging system.

AKAR Reporter Assays. The HeLa cells utilized for these experiments were between passages 60 and 61. Cells were maintained in DMEM growth media supplemented with 10% FBS and 1% penicillin and streptomycin. They were transfected with the appropriate biosensor at an approximate confluency of 70% using Lipofectamine 2000 reagent and incubated for 24 h. Prior to imaging, cells were pretreated with 5 μM active or control peptides at 37 °C in DMEM for 6 h. They were then imaged in HBSS buffer supplemented with the corresponding peptide at RT.

Epifluorescence imaging was performed on a Zeiss Axiovert 200 M Microscope equipped with a xenon lamp and a cooled CCD, under a 40X oil immersion objective. FRET microscopy of CFP/YFP biosensors was performed using the following excitation/emission filter combinations (bandwidths in nm): CFP: Ex 420/20, Em 475/40; YFP: Ex 495/10, Em 535/25; FRET: Ex 420/20, Em 535/25. All epifluorescence experiments were subsequently analyzed using the MetaFluor software. All cells were analyzed, including those with visible blebbing or other morphological defects. Such cells typically present problems such as biosensor leakage and did not accurately reflect activity. They were therefore rejected from reporting. The reported FRET ratio is calculated as follows and normalized with respect to the first frame in the time series (I = intensity):

$$\frac{I_{\text{FRET}} - I_{\text{FRET,background}}}{I_{\text{CFP}} - I_{\text{CFP,background}}}$$

ASSOCIATED CONTENT

Ⓢ Supporting Information

This material is available free of charge via the Internet at http://pubs.acs.org.

AUTHOR INFORMATION

Corresponding Author

*E-mail: ekennedy@uga.edu.

Notes

The authors declare no competing financial interest.

ACKNOWLEDGMENTS

REFERENCES

(1) Taylor, S. S., Ilouz, R., Zhang, P., and Kornev, A. P. (2012) Assembly of allosteric macromolecular switches: lessons from PKA. *Nat. Rev. Mol. Cell Biol. 13*, 646−658.

(2) Taylor, S. S., Zhang, P., Steichen, J. M., Keshwani, M. M., and Kornev, A. P. (2013) PKA: lessons learned after twenty years. *Biochim. Biophys. Acta 1834*, 1271−1278.

(3) Welch, E. J., Jones, B. W., and Scott, J. D. (2010) Networking with AKAPs: context-dependent regulation of anchored enzymes. *Mol. Interventions 10*, 86−97.

(4) Johnson, D. A., Akamine, P., Radzio-Andzelm, E., Madhusudan, M., and Taylor, S. S. (2001) Dynamics of cAMP-dependent protein kinase. *Chem. Rev. 101*, 2243−2270.

(5) Herberg, F. W., Taylor, S. S., and Dostmann, W. R. (1996) Active site mutations define the pathway for the cooperative activation of cAMP-dependent protein kinase. *Biochemistry 35*, 2934−2942.

(6) Skroblin, P., Grossmann, S., Schafer, G., Rosenthal, W., and Klussmann, E. (2010) Mechanisms of protein kinase A anchoring. *Int. Rev. Cell Mol. Biol. 283*, 235−330.

(7) Dessauer, C. W. (2009) Adenylyl cyclase—A-kinase anchoring protein complexes: the next dimension in cAMP signaling. *Mol. Pharmacol. 76*, 935−941.

(8) Sanderson, J. L., and Dell'Acqua, M. L. (2011) AKAP signaling complexes in regulation of excitatory synaptic plasticity. *Neuroscientist 17*, 321−336.

(9) Diviani, D., Dodge-Kafka, K. L., Li, J., and Kapiloff, M. S. (2011) A-kinase anchoring proteins: scaffolding proteins in the heart. *Am. J. Physiol. Heart Circ. Physiol. 301*, H1742−1753.

(10) Gold, M. G., Lygren, B., Dokurno, P., Hoshi, N., McConnachie, G., Tasken, K., Carlson, C. R., Scott, J. D., and Barford, D. (2006) Molecular basis of AKAP specificity for PKA regulatory subunits. *Mol. Cell 24*, 383−395.

(11) Herberg, F. W., Maleszka, A., Eide, T., Vossebein, L., and Tasken, K. (2000) Analysis of A-kinase anchoring protein (AKAP) interaction with protein kinase A (PKA) regulatory subunits: PKA isoform specificity in AKAP binding. *J. Mol. Biol. 298*, 329−339.

(12) Burgers, P. P., Ma, Y., Margarucci, L., Mackey, M., van der Heyden, M. A., Ellisman, M., Scholten, A., Taylor, S. S., and Heck, A. J. (2012) A small novel A-kinase anchoring protein (AKAP) that localizes specifically protein kinase A-regulatory subunit I (PKA-RI) to the plasma membrane. *J. Biol. Chem. 31*, 31.

(13) Troger, J., Moutty, M. C., Skroblin, P., and Klussmann, E. (2012) A-kinase anchoring proteins as potential drug targets. *Br. J. Pharmacol. 29*, 1476−5381.

(14) Carnegie, G. K., Means, C. K., and Scott, J. D. (2009) A-kinase anchoring proteins: from protein complexes to physiology and disease. *IUBMB Life 61*, 394−406.

(15) Blant, A., and Czubryt, M. P. (2012) Promotion and inhibition of cardiac hypertrophy by A-kinase anchor proteins. *Can. J. Physiol. Pharmacol. 90*, 1161−1170.

(16) Carr, D. W., Hausken, Z. E., Fraser, I. D., Stofko-Hahn, R. E., and Scott, J. D. (1992) Association of the type II cAMP-dependent protein kinase with a human thyroid RII-anchoring protein. Cloning and characterization of the RII-binding domain. *J. Biol. Chem. 267*, 13376−13382.

(17) Carlson, C. R., Lygren, B., Berge, T., Hoshi, N., Wong, W., Tasken, K., and Scott, J. D. (2006) Delineation of type I protein kinase A-selective signaling events using an RI anchoring disruptor. *J. Biol. Chem. 281*, 21535−21545.

(18) Vijayaraghavan, S., Goueli, S. A., Davey, M. P., and Carr, D. W. (1997) Protein kinase A-anchoring inhibitor peptides arrest mammalian sperm motility. *J. Biol. Chem. 272*, 4747−4752.

641

dx.doi.org/10.1021/cb400900r | *ACS Chem. Biol.* 2014, 9, 635−642

(19) Nakase, I., Takeuchi, T., Tanaka, G., and Futaki, S. (2008) Methodological and cellular aspects that govern the internalization mechanisms of arginine-rich cell-penetrating peptides. *Adv. Drug Delivery Rev. 60*, 598−607.

(20) Patel, H. H., Hamuro, L. L., Chun, B. J., Kawaraguchi, Y., Quick, A., Rebolledo, B., Pennypacker, J., Thurston, J., Rodriguez-Pinto, N., Self, C., Olson, G., Insel, P. A., Giles, W. R., Taylor, S. S., and Roth, D. M. (2010) Disruption of protein kinase A localization using a trans-activator of transcription (TAT)-conjugated A-kinase-anchoring peptide reduces cardiac function. *J. Biol. Chem. 285*, 27632−27640.

(21) Verdine, G. L., and Hilinski, G. J. (2012) Stapled peptides for intracellular drug targets. *Methods Enzymol. 503*, 3−33.

(22) Verdine, G. L., and Walensky, L. D. (2007) The challenge of drugging undruggable targets in cancer: lessons learned from targeting BCL-2 family members. *Clin. Can. Res. 13*, 7264−7270.

(23) Burns-Hamuro, L. L., Hamuro, Y., Kim, J. S., Sigala, P., Fayos, R., Stranz, D. D., Jennings, P. A., Taylor, S. S., and Woods, V. L., Jr. (2005) Distinct interaction modes of an AKAP bound to two regulatory subunit isoforms of protein kinase A revealed by amide hydrogen/deuterium exchange. *Protein Sci. 14*, 2982−2992.

(24) Kinderman, F. S., Kim, C., von Daake, S., Ma, Y., Pham, B. Q., Spraggon, G., Xuong, N. H., Jennings, P. A., and Taylor, S. S. (2006) A dynamic mechanism for AKAP binding to RII isoforms of cAMP-dependent protein kinase. *Mol. Cell 24*, 397−408.

(25) Sarma, G. N., Kinderman, F. S., Kim, C., von Daake, S., Chen, L., Wang, B. C., and Taylor, S. S. (2010) Structure of D-AKAP2:PKA RI complex: insights into AKAP specificity and selectivity. *Structure 18*, 155−166.

(26) Schafmeister, C. E., Po, J., and Verdine, G. L. (2000) An all-hydrocarbon cross-linking system for enhancing the helicity and metabolic stability of peptides. *J. Am. Chem. Soc. 122*, 5891−5892.

(27) Blackwell, H. E., Sadowski, J. D., Howard, R. J., Sampson, J. N., Chao, J. A., Steinmetz, W. E., O'Leary, D. J., and Grubbs, R. H. (2001) Ring-closing metathesis of olefinic peptides: design, synthesis, and structural characterization of macrocyclic helical peptides. *J. Org. Chem. 66*, 5291−5302.

(28) Bertinetti, D., Schweinsberg, S., Hanke, S. E., Schwede, F., Bertinetti, O., Drewianka, S., Genieser, H. G., and Herberg, F. W. (2009) Chemical tools selectively target components of the PKA system. *BMC Chem. Biol. 9*, 3.

(29) Friedrich, M. W., Aramuni, G., Mank, M., Mackinnon, J. A., and Griesbeck, O. (2010) Imaging CREB activation in living cells. *J. Biol. Chem. 285*, 23285−23295.

(30) Depry, C., Allen, M. D., and Zhang, J. (2011) Visualization of PKA activity in Plasma Membrane Microdomains. *Mol. BioSyst. 7* (1), 52−58.

(31) Banky, P., Newlon, M. G., Roy, M., Garrod, S., Taylor, S. S., and Jennings, P. A. (2000) Isoform-specific differences between the type Ialpha and IIalpha cyclic AMP-dependent protein kinase anchoring domains revealed by solution NMR. *J. Biol. Chem. 275*, 35146−35152.